mmol) of pyridine in 1.28 mL of dichloromethane, and the resulting solution was stirred for 10 min at room temperature. A solution of ketal **33** (57.0 mg, 0.128 mmol) dissolved in 2 mL of dichloromethane and acetic anhydride (48.3 μL, 0.512 mmol) was then added sequentially to this mixture. After 10 min, the reaction mixture was transferred to a silica gel column, and the column was eluted with 50% ethyl acetate-hexane to give 28.8 mg (51%) of the β-keto lactone **34** as a colorless solid: $[\alpha]^{24}_D$ +60.80 (*c* 1.44, $CHCl_3$); IR (neat) 3310, 2940, 2865, 1715, 1650, 1595, 1530, 1455, 1420, 1395, 1361, 1345, 1270, 1225, 1165, 1115, 1055, 905, 735, 700 cm^{-1}; ^1H NMR ($CDCl_3$) δ 11.98 (s, 1 H), 7.34 (s, 5 H), 5.19 (d, 1 H, *J* = 12.1 Hz), 5.07 (d, 1 H, *J* = 12.1 Hz), 4.71 (d, 1 H, *J* = 10.1 Hz), 4.59 (q, 1 H, *J* = 6.5 Hz), 4.35 (d, 2 H, *J* = 10.1 Hz), 3.71 (ddd, 1 H, *J* = 11.1, 9.4, 6.1 Hz), 3.30 (t, 1 H, *J* = 9.4 Hz), 2.98-2.85 (m, 2 H), 2.58 (ddd, 1 H, *J* = 17.4, 11.1, 2.6 Hz), 1.70-1.50 (m, 10 H), 1.37 (d, 3 H, *J* = 6.5 Hz); exact mass calcd for $C_{24}H_{29}NO_7$ 443.1935, found 443.1935. Anal. Calcd for $C_{24}H_{29}NO_7$: C, 65.00; H, 6.59; N, 3.16. Found: C, 64.84; H, 6.93; N, 2.95.

Protected Actinobolin 35. To a solution of 14.0 mg (0.032 mmol) of **34** in 1.5 mL of dichloromethane was added 10 mg of 5% palladium on carbon. The mixture was stirred under an atmosphere of hydrogen gas for I h. The catalyst was removed by filtration, and to the resulting filtrate were added 8.5 mg (0.038 mmol) of *N*-carbobenzoxy-L-alanine and 7.8 mg (0.038 mmol) of 1,3-dicyclohexylcarbodiimide. The mixture was stirred for 1 h and filtered. The filtrate was chromatographed on silica gel with ethyl acetate-hexane as the eluent to give 14.7 mg (90%) of protected actinobolin **35** as a colorless solid: $[\alpha]^{24}_D$ +15.1° (*c* 0.74, $CHCl_3$); IR (neat) 3310, 2940, 2865, 1725, 1680, 1645, 1590, 1535, 1450, 1420, 1395, 1360, 1345, 1270, 1230, 1115, 1075, 1055, 905, 755 cm^{-1}; ^1H NMR ($CDCl_3$) δ 13.68 (s, 1 H), 7.34 (s, 5 H), 6.45 (br d, 1 H, *J* = 8.0 Hz), 5.32 (d, 1 H, *J* = 6.8 Hz), 5.09 (d, 1 H, *J* = 11.8), 5.50 (d, 1 H, *J* = 11.8 Hz), 4.67-4.56 (m, 2 H), 4.26 (quintet, 1 H, *J* = 7.0 Hz), 3.70 (ddd, 1 H, *J* = 11.2, 9.3, 6.1 Hz), 3.31 (t, 1 H, *J* = 9.30 Hz), 2.99-2.87 (m, 2 H), 2.59 (ddd, 1 H, *J* = 16.7, 11.2, 2.0 Hz), 1.75-1.55 (m, 10 H), 1.39 (d, 3 H, *J* = 7.0 Hz), 1.30 (d, 3 H, *J* = 6.5 Hz); exact mass calcd for $C_{27}H_{34}N_2O_8$ 514.2316, found 514.2301. Anal. Calcd for $C_{27}H_{34}N_2O_8$: C, 63.02; H, 6.66; N, 5.45. Found: C, 62.90; H, 6.70; N, 5.28.

[3*R*-(3α,4α(*S)4α,5α,6α)]-2-Amino-*N*-(3,4,4a,5,6,7-hexahydro-5,6,8-trihydroxy-3-methyl-1-oxo-1*H*-2-benzopyran-4-yl)propanamide Monohydrochloride (1·HCl).** A mixture of 15.7 mg (0.0305 mmol) of **35**, 0.63 mL of methanol, 0.063 mL of acetic acid, 0.091 mL of 1 N hydrochloric acid, and 5 mg of 5% palladium on carbon was stirred under a hydrogen atmosphere at room temperature for 30 min. The catalyst was removed by filtration, and the filtrate was concentrated in vacuo to dryness. The resulting oil was triturated twice with 1 mL of anhydrous ether to give a pale yellow solid. The solid was dissolved in 3 mL of water and filtered. The filtrate was freeze-dried under reduced pressure to give 10.5 mg (100%) of actinobolin hydrochloride as a pale yellow powder: $[\alpha]^{24}_D$ +50° (*c* 0.52, H_2O); IR (KBr) 3410, 1650, 1560, 1505, 1395, 1265, 1230, 1190, 1135, 1110, 1085, 1070, 1050, 1005, 805, 760, 710 cm^{-1}; ^1H NMR (CD_3OD, Me_4Si standard) 4.70 (qd, 1 H, *J* = 6.41, 1.3 Hz), 4.57 (m, 1 H), 4.03 (q, 1 H, *J* = 7.0 Hz), 3.88 (td, 1 H, *J* = 9.6, 6.7 Hz), 3.13 (t, 1 H, *J* = 9.6 Hz), 2.84-2.75 (m, 2 H), 2.36 (ddd, 1 H, *J* = 18.6, 9.6, 2.4 Hz), 1.51 (d, 3 H, *J* = 7.0 Hz), 1.34 (d, 3 H, *J* = 6.4 Hz).

Preparation of an Authentic Sample of Actinobolin Hydrochloride 16 from Actinobolin Sulfate. A column packed with 10 mL of Amberlite IRA 400 (Cl form) was washed with 5 mL of hydrochloric acid and then with enough water to bring the pH of the eluent to 7. The column was charged with natural actinobolin sulfate (10 mg) and dissolved in 0.5 mL of water, and the column was eluted with water. The fractions containing actinobolin hydrochloride (ascertained by silica gel TLC analysis using acetonitrile-water-acetic acid (5:1:1) as the developing solvent) were collected, combined, and freeze-dried under reduced pressure to give 9.2 mg of actinobolin hydrochloride: $[\alpha]^{24}_D$ +53° (*c* 0.65, H_2O). Actinobolin was isolated from its sulfate salt by neutralization with aqueous sodium bicarbonate and extraction with 2-butanone. MS (15 eV), *m/e* 264 (M^+-2H_2O), 220, 202, 170, 162; exact mass calcd for $C_{13}H_{16}N_2O_4$ 264.1111, found 264.1102.

Acknowledgment. We are indebted to the American Cancer Society (Grant No. CH-249) for its generous support of these studies. We thank Dr. Martin Black of the Warner-Lambert Company for the authentic sample of actinobolin.

Supplementary Material Available: Tables containing the final fractional coordinates, temperature parameters, bond distances, and bond angles for **16b** (4 pages). Ordering information is given on any current masthead page.

Fluorescence and Photoisomerization of Azobenzene-Containing Bilayer Membranes

Masatsugu Shimomura[1] and Toyoki Kunitake*

Contribution No. 804 from the Department of Organic Synthesis, Faculty of Engineering, Kyushu University, Fukuoka 812, Japan. *Received December 23, 1986*

Abstract: Spectroscopic and photoisomerization behavior of aqueous bilayer aggregates of azobenzene-containing amphiphiles was examined. The azobenzene bilayers assume different chromophore orientations, depending on the component structure. Some of the azobenzene bilayers were found to be fluorescent, and the fluorescence intensity decreased as the chromophore orientation changed from the tilted head-to-tail type to the parallel type. Emission quenching was observed in the presence of extremely small amounts of a bound cyanine dye. In the trans-to-cis photoisomerization of the bilayers, the rate in the gel state decreased with changing chromophore orientations from the head-to-tail type to the parallel type. The rate was much larger and unaffected by the molecular structure, in the case of the liquid-crystalline bilayers and of the azobenzene amphiphiles isolated in inert bilayer matrices. In the phase-separated system, photoisomerization occurred between the unclustered isomers. The emission was quickly lost by the formation of the cis isomer. The photoisomerization was suppressed in the presence of the cyanine, probably due to energy transfer to the cyanine and sensitization of the reverse photoisomerization by the cyanine. An energy level diagram was constructed which includes excited states characteristic of the bilayer and explains the photophysical and photochemical processes. Finally, implications of the present finding in relation to light energy harvesting systems were discussed.

We have been investigating in the past several years spontaneous assemblage of bilayers in water from amphiphiles which contain aromatic segments.[2] In these bilayers, spectral properties of the aromatic units are extensively affected by the chemical structure of component molecules and by the physical state of membranes, due to the electronic interaction of the aromatic units.[3-7] In

(1) Present address: Department of Industrial Chemistry, Faculty of Technology, Tokyo University of Agriculture and Technology, Koganei 184, Japan

(2) Kunitake, T.; Okahata, Y.; Shimomura, M.; Yasunami, S.; Takarabe, K. *J. Am. Chem. Soc.* **1981**, *103*, 5401-5413.

0002-7863/87/1509-5175$01.50/0

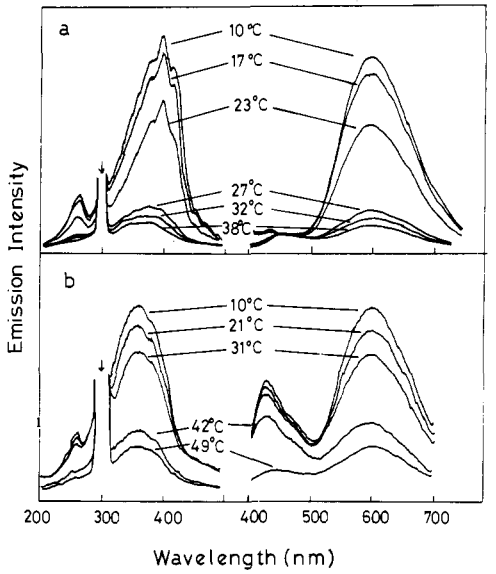

Figure 1. Emission and excitation spectra of aqueous bilayers of azobenzene-containing bilayer membranes. (a) $[C_{12}AzoC_5N^+] = 4.5 \times 10^{-4}$ M. Emission spectra are obtained by excitation at 380 nm, and excitation spectra are monitored at 600 nm. (b) $[C_{12}AzoC_6N^+] = 3.5 \times 10^{-4}$ M. Excitation at 360 nm. Excitation spectra monitored at 600 nm.

particular, the molecular structure of component amphiphiles was systematically varied in the case of azobenzene-containing amphiphiles, and absorption spectra of the bilayer membranes thereof were examined in detail.[6]

Absorption spectra of isolated azobenzene amphiphiles $C_nAzoC_mN^+$ **1** (e.g., dissolved in ethanol) possess λ_{max} at 355 nm, without regard to methylene chain lengths of the tail (C_n) and spacer (C_m) portions. When these amphiphiles form bilayer

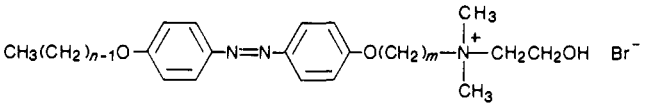

$C_nAzoC_mN^+$ (1)

membranes in water, absorption maxima exhibit extensive shifts in the region of 300–400 nm, depending on the alkyl chain length and temperature. A semiquantitative application of Kasha's molecular exciton theory[8] suggests that the bathochromic shift is derived from the head-to-tail orientation of the transition dipole of the long axis of the chromophore. On the other hand, the hypsochromic shift is attributable to the parallel orientation of the transition dipole. Some of these structural inferences were verified by the X-ray structural analysis of cast films and single crystals.[9,10]

Supposing that the Davydov splitting is responsible for the observed spectral variation, the excitonic state as in molecular crystals[11] may be produced in the ordered azobenzene assembly, and physical and chemical characteristics due to the long-distance interaction of the chromophore will be observed. We have briefly reported photoisomerization of azobenzene bilayers and the consequent changes in morphology[3] and permeability.[12] The subsequent study, however, indicated that the photoprocess in the bilayer was not necessarily straightforward, and we set out to carry out a systematic study. In this article, we report enhanced luminescence from azobenzene bilayer assemblies and efficient energy transfer to a cyanine dye bound at the membrane surface. The cis–trans photoisomerization of component azobenzenes is affected by the mode of the chromophore interaction and by sensitization. These results will be useful for developing ways to control the photochemical reactivity and energy transfer in the bilayer assembly.

Experimental Section

Materials. The preparation of the azobenzene amphiphiles **1**[6] and double-chain ammonium amphiphiles **2**[13,14] have been reported elsewhere. Cyanine dye **3** (Nippon Kanko Shikiso, NK 2012) was used without further purification. Solvents used for fluorometry were those of the

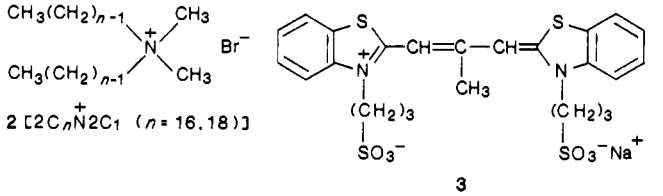

3

spectrophotometric grade: ethanol (Merk UVasole) and 2-propanol (Nakarai Chemicals.). Freshly distilled, deionized water was used for spectroscopic measurements.

Preparation of Aqueous Bilayer Dispersions. Transparent stock solutions of single-component bilayers (10 mM) were prepared by sonication with a Bransonic Cell Disruptor 185. Aqueous solutions of mixed bilayers were obtained by mixing necessary amounts of two stock solutions and by the subsequent sonication. In both single-component and mixed-component solutions, the concentration of the azobenzene amphiphile was adjusted to ca. 0.4 mM by dilution.

Spectral Measurements. Absorption spectra were obtained with Hitachi 200 or 220A spectrophotometers equipped with constant-temperature cell holders. Fluorescence spectra were measured with a Hitachi 650-60 spectrofluorimeter equipped with a Hamamatsu Photonics R298F photomultiplier and a constant-temperature cell holder. One-millimeter quartz cells were used in most cases in order to avoid self-absorption. The spectra obtained were corrected at 280–600 nm by the microprocessor-operated correction mode, using Rhodamine B as quantum counter. Quinine sulfate was used for calculation of the relative quantum efficiency.

Photoisomerization. A 150-W Xenon lamp of a Hitachi 650 spectrofluorimeter was used as the light source for the photoisomerization of azobenzenes. The monochromatic light at 360 nm was used for the trans-to-cis isomerization, because absorbances of the trans isomers are large and those of the cis isomers are relatively small at this wavelength. In the cis-to-trans photoisomerization, the monochromatic light at 450 nm was used to directly excite the n–π^* transition of the cis isomer. The 580-nm light was used to excite the bound cyanine dye together with a Toshiba L-42 filter which eliminates light at wavelengths shorter than 420 nm.

Results

Fluorescence of Azobenzene-Containing Bilayers. During the course of the study on photoisomerization, an aqueous dispersion of the azobenzene bilayer was accidentally found to be luminescent under irradiation at 360 nm. As discussed later, the emission is considered to be fluorescence rather than phosphorescence. Figure 1 demonstrates emission and excitation spectra of aqueous bilayers of $C_{12}AzoC_5N^+$ and $C_{12}AzoC_6N^+$. A broad emission is observed for the $C_{12}AzoC_5N^+$ bilayer (Figure 1a) at ca. 600 nm (uncorrected) with excitation at 400 nm. A weak emission peak is also seen at ca. 420 nm. An excitation spectrum monitored at 600 nm gives structured peaks centered at ca. 380 nm at 10–20 °C.

(3) Kunitake, T.; Okahata, Y.; Nakashima, N.; Shimomura, S.; Kano, K.; Ogawa, T. *J. Am. Chem. Soc.* **1980**, *102*, 6642–6644.
(4) Kunitake, T.; Nakashima, N.; Morimitsu, K. *Chem. Lett.* **1980**, 1347–1350.
(5) Shimomura, M.; Hashimoto, H.; Kunitake, T. *Chem. Lett.* **1982**, 1285–1288.
(6) Shimomura, M.; Ando, R.; Kunitake, T. *Ber. Bunsenges. Phys. Chem.* **1983**, *87*, 1134–1143.
(7) Kunitake, T.; Tawaki, S.; Nakashima, N. *Bull. Chem. Soc. Jpn.* **1983**, *56*, 3235–3242.
(8) McRae, E. G.; Kasha, M. In *Physical Processes in Radiation Biology*; Academic: New York, 1964; p 23.
(9) Kunitake, T.; Shimomura, M.; Kajiyama, T.; Harada, A.; Okuyama, K.; Takayanagi, M. *Thin Solid Films* **1984**, *121*, L89–L91.
(10) Okuyama, K.; Watanabe, H.; Shimomura, M.; Hirabayashi, H.; Kunitake, T.; Kajiyama, T.; Yasuoka, N. *Bull. Chem. Soc. Jpn.* **1986**, *59*, 3351–3356.
(11) Davydov, A. S. *Theory of Molecular Excitons*; translated by Kasha, M., Oppenheimer, M.; McGraw-Hill: New York, 1962.
(12) Kano, K.; Tanaka, Y.; Ogawa, T.; Okahata, Y.; Kunitake, T. *Chem. Lett.* **1980**, 421–424. Kano, K.; Tanaka, Y.; Ogawa, T.; Shimomura, M.; Kunitake, T. *Photochem. Photobiol.* **1981**, *34*, 323–329.
(13) Kunitake, T.; Okahata, Y.; Tamaki, K.; Kumamaru, F.; Takayanagi, M. *Chem. Lett.* **1977**, 387–390.
(14) Okahata, Y.; Ihara, H.; Kunitake, T. *Bull. Chem. Soc. Jpn.* **1981**, *54*, 2072–2078.

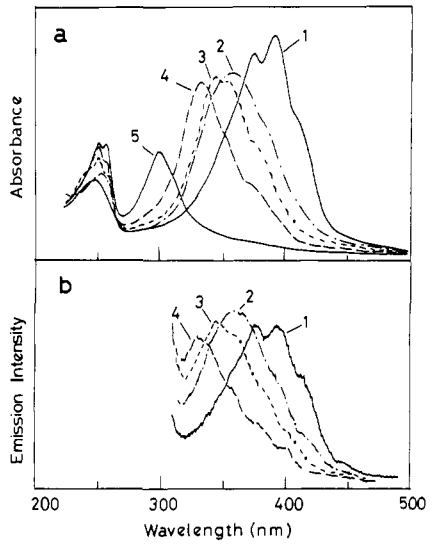

Figure 2. Comparison of absorption (a) and excitation (b) spectra of aqueous bilayers. Bilayer membranes, 1.0×10^{-4} M; 10 °C. Excitation spectra are monitored at 600 nm and their intensities are normalized. (1) $C_{12}AzoC_5N^+$ (the $C_{10}AzoC_5N^+$ bilayer gives identical spectra); (2) $C_{12}AzoC_4N^+$; (3) $C_{12}AzoC_6N^+$; (4) $C_{10}AzoC_{10}N^+$; (5) $C_8AzoC_{10}N^+$.

Its lifetime is estimated to be in the picosecond range, since the decay cannot be detected by an Ortec PRA single-photon counter (pulse resolution, 2 ns).[15] The very short lifetime suggests that the emission is due to fluorescence from the excited singlet state. An approximate quantum yield is calculated to be 10^{-3} by using quinine sulfate as a standard. The spectral correction is not possible with our instrument at wavelengths beyond 600 nm, and therefore, the quantum yield could not be determined more accurately.

Similar results are obtainable for the $C_{12}AzoC_6N^+$ bilayer, though the 420-nm emission is stronger (Figure 1b).

The fluorescence spectra are dependent on temperature. The spectral intensities are drastically lessened at higher temperatures. The decrease is most pronounced at 23–27 °C for $C_{12}AzoC_5N^+$. This temperature range corresponds approximately to the lower half of the DSC peak (heating scan) of the crystal-to-liquid crystal-phase transition.[6] In the case of the aqueous $C_{12}AzoC_6N^+$ bilayer, the intensities of its emission and excitation spectra are drastically lessened at 30–40 °C, in agreement with its T_c (28 °C). Strong luminescence is recovered by lowering the temperature.

Figure 2 displays the correspondence between absorption and excitation spectra of several azobenzene bilayers. As discussed already, the absorption spectrum varies extensively with the methylene chain length in the tail and spacer portions. The emission intensities are normalized. Fairly strong fluorescence is observed for the bilayers of $C_{12}AzoC_5N^+$, $C_{10}AzoC_5N^+$, and $C_{12}AzoC_4N^+$, and weaker fluorescence is found for the bilayers of $C_{12}AzoC_6N^+$ and $C_{10}AzoC_{10}N^+$. No luminescence is observed for the $C_8AzoC_{10}N^+$ bilayer which possesses the absorption maximum at 300 nm.

The corrected excitation spectra of Figure 2b are very similar in peak positions and shapes to the absorption spectra of the corresponding bilayers of Figure 2a. Undoubtedly, the observed fluorescence is ascribable to excitation of the azobenzene chromophore. In all cases (Figures 1 and 2), fluorescence is not detected when azobenzene amphiphiles are dissolved in ethanol or in 2-propanol or when they are molecularly dispersed in the bilayer matrix of $2C_{16}N^+2C_1$. Immediately after a 2-propanol solution of $C_{10}AzoC_5N^+$ is quenched to −65 °C, no emission is observed. Emission is gradually intensified along with the formation of azobenzene microcrystals from the supercooled solution.

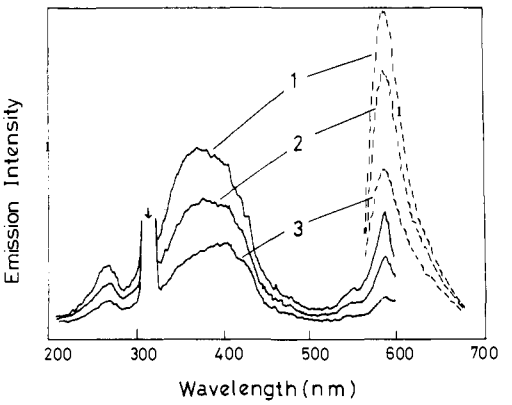

Figure 3. Excitation and emission spectra of the $C_{12}AzoC_5N^+$ bilayer in the presence of a bound cyanine dye. Excitation spectra (solid line) are monitored at 610 nm and emission spectra (dotted line) are obtained by excitation at 370 nm. $[C_{12}AzoC_5N^+] = 3.5 \times 10^{-4}$ M, 10 °C. The concentrations of cyanine dye **3** are 1.2×10^{-8} M (1), 1.2×10^{-9} M (2), and 1.2×10^{-10} M (3).

Its excitation spectrum agrees with the absorption spectrum (λ_{max} 390 nm). These data strongly indicate that the crystalline aggregation of the azobenzene amphiphiles is required for efficient fluorescence.

Fluorescence Quenching by Membrane-Bound Cyanine Dye. The data of Figures 1 and 2 indicate that strong fluorescence is observed for the bathochromic azobenzene bilayers. Since the bathochromism (and hypsochromism) is considered to be a result of Davydov splitting, the observed fluorescence is ascribable to the existence of the excitonic state in the bilayer assembly. This possibility can be examined by the energy-transfer experiment to added acceptors: e.g., tetracene doped in the single crystal of anthracene.[16]

Anionic cyanine dye **3** is efficiently bound to ammonium bilayer membranes, resulting in a bathochromic shift of the absorption spectrum and strong fluorescence with a small Stokes shift.[17] These spectral data suggest the formation of "J aggregate" at the membrane surface. The emission maximum from the $C_{12}AzoC_5N^+$ bilayer is located at 600 nm, and the energy acceptor for this bilayer must absorb in this region. Cyanine dye **3** is suitable for this purpose, because it absorbs at 580 nm when bound to the $C_{12}AzoC_5N^+$ bilayer, but not in the 300–500 nm region where the azobenzene chromophore absorbs.

Figure 3 illustrates fluorescence spectra of the $C_{12}AzoC_5N^+$ bilayer loaded with cyanine dye **3**. Excitation at 360 nm produces sharp emission at 580 nm in place of a broad 600-nm peak characteristic of the azobenzene fluorescence. The sharp, intensified peak is indicative of the cyanine *J* aggregate. Since the cyanine dye does not absorb at 360 nm, the excitation energy must be transferred from the azobenzene. The excitation spectrum monitored at 610 nm shows two peaks due to the azobenzene moiety (360 nm) and the cyanine dye (580 nm). It should be emphasized that the cyanine fluorescence is observable at 1.2×10^{-10} M. This is *one three millionth* of the azobenzene concentration and indicates that the energy transfer is unusually effective.

Similar energy-transfer phenomena are observed for bilayers of $C_{12}AzoC_6N^+$ and $C_{10}AzoC_{10}N^+$. The emission intensity without cyanine increases in the order of $C_{12}AzoC_5N^+$ (1.0) > $C_{12}AzoC_6N^+$ (0.3) > $C_{10}AzoC_{10}N^+$ (0.2). The number in parentheses gives the approximate relative intensity. This order agrees with that of bathochromicity (red shift) in the absorption spectrum and indicates that the formation of the *J* aggregate (the head-to-tail orientation of the azobenzene) facilitate the emission. The emission intensity of the cyanine increases with increasing cyanine concentrations in any of the azobenzene bilayers. The relative intensity among the different systems becomes close to each other

(15) We thank Dr. K. Kano of Doshisha University for the use of the instrument. A more recent picosecond study at the Institute for Molecular Science, Okazaki, Japan, confirmed that this is in fact the case.

(16) Benz, K. W.; Wolf, H. C. *Z. Naturforsch.* **1964**, *19a*, 177–190.
(17) Nakashima, N.; Kunitake, T. *J. Am. Chem. Soc.* **1982**, *104*, 4261–4262.

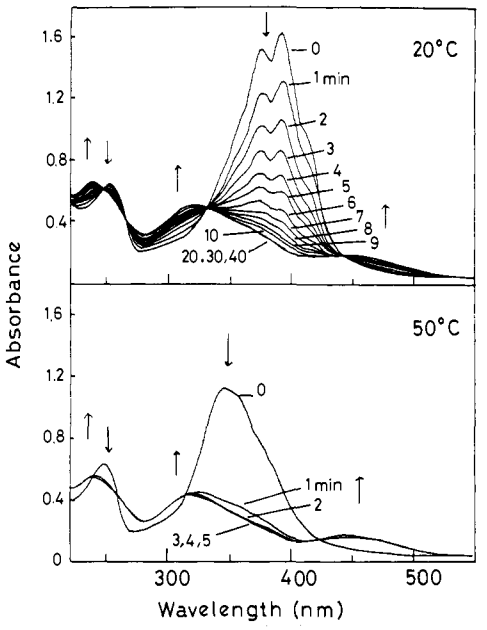

Figure 4. Changes of absorption spectra due to the trans-to-cis photoisomerization. $[C_{12}AzoC_5N^+] = 3.8 \times 10^{-4}$ M. Irradiation at 360 nm.

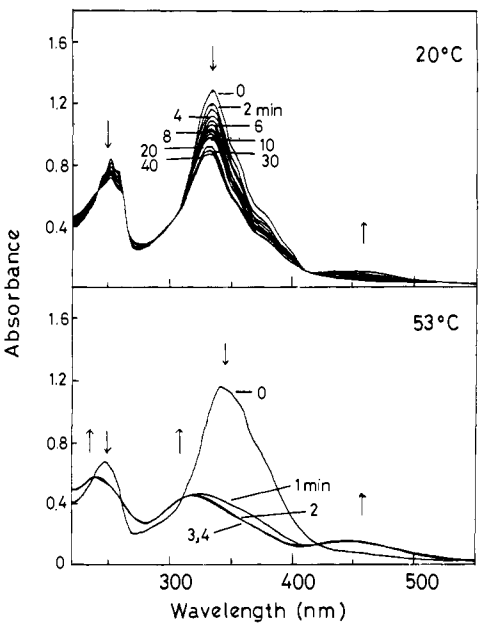

Figure 5. Changes of absorption spectra due to the trans-to-cis photoisomerization. $[C_{10}AzoC_{10}N^+] = 4.0 \times 10^{-4}$ M. Irradiation at 360 nm.

at high cyanine concentrations.

Interestingly, the cyanine dye does not form *J* aggregates when bound to the $C_8AzoC_{10}N^+$ bilayer that does not fluoresce. In this case the membrane-bound cyanine gives a sharp absorption maximum at 505 nm due to formation of the H aggregate (parallel chromophore stacking), subsequent to a complex spectral change with time. We reported previously for other bilayer systems that emission from this type of dye aggregate is very weak.[17,18]

The cyanine emission is not particularly sensitive to the physical state of the azobenzene bilayer. The intensity of the emission from the $C_{12}AzoC_5N^+$ bilayer containing $1/10^4$ mol/mol of the cyanine is little affected by temperature between 10 and 37 °C, in spite of the fact that the emission from the azobenzene bilayer itself is much diminished near the phase transition temperature (32 °C) as shown in Figure 1. The cyanine dye collects efficiently the excitation energy absorbed by the azobenzene bilayer without regard to its physical state.

Photochemical Cis–Trans Isomerization of the Azobenzene Bilayer. The photochemical process of the azobenzene bilayers would be strongly influenced by their peculiar photophysical behavior discussed above: formation of the excitonic state and efficient energy transfer to the bound cyanine. In general, the excitation energy of *trans*-azobenzenes is partly consumed by the isomerization and the rest is lost thermally. The nature of the excited state should be rather different between the isolated species and the bilayer assembly. The investigation of the photochemical behavior gives additional information on the fate of excitation energy.

The three azobenzene amphiphiles employed for the isomerization study are those that display largest spectral shifts in the form of the bilayer assembly. Figure 4 demonstrates absorption spectral changes of the $C_{12}AzoC_5N^+$ bilayer due to photoisomerization. Upon irradiation, the peak intensity of the crystalline bilayer (e.g., at 20 °C) decreases and, in its place, new peaks appear at 450 and 320 nm which are ascribable to the $n-\pi^*$ and $\pi-\pi^*$ transitions, respectively, of the cis isomer. The spectral change is complete in 20 min and further irradiation (30 and 40 min) is not effective. In contrast, when the bilayer is in the liquid-crystalline state at 50 °C, its absorption maximum is located at 340 nm, and the photostationary state is attained in only 2 min upon irradiation at 360 nm.

Figure 5 shows the spectral change of the $C_{10}AzoC_{10}N^+$ bilayer. The photoisomerization is very slow at 20 °C, and the photostationary state is apparently not attained even after 40 min. On the other hand, it is attained in as fast as 2 min at 53 °C where the bilayer is in the liquid-crystalline state and absorbs at 340 nm. Interestingly, the $C_8AzoC_{10}N^+$ bilayer which displays the largest blue shift at 300 nm does not give any spectral change in the crystalline state (25 °C) upon 360-nm irradiation.

The rate of photoisomerization depends on light intensity and absorbance at the irradiating wavelength. In the present experiments, the same spectrofluorimeter is employed throughout and the reaction rates are reproducible. Therefore, the light intensities are conceivably not varied under the identical conditions, although they are not determined in each experiment. The amount of light absorbed in each bilayer can therefore be estimated on the basis of the respective absorbance at irradiating wavelengths which vary with compounds and the experimental conditions.

The relative absorbances at 360 nm of the three bilayers ($C_{12}AzoC_6N^+$, $C_{10}AzoC_{10}N^+$, and $C_8AzoC_{10}N^+$) are 1:0.64:0.14 at 20 °C. If the reaction rate is simply proportional to the amount of absorbed light, its ratio should coincide with the relative absorbance. However, the decreases in the trans isomer after 10 min of irradiation as determined by eq 1 (see below) are respectively 82%, 23%, and 0%, and their ratio (1:0.28:0) does not agree with the relative absorbance.

We reported in a previous publication[3] that the decrease in the *trans*-azobenzene unit in bilayer **4** in the photostationary state (500-W Hg lamp, UV D35 filter) is enhanced from 20% at 40 °C to 50% at 50 °C, as the physical state of the bilayer changes (T_c = 45 °C). However, under the conditions used in this study,

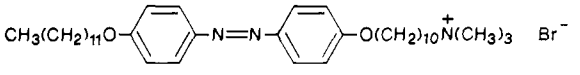

4

the photostationary state is attained only after much longer irradiation, and the fraction of the cis isomer is not affected by the bilayer physical state (phase transition). Therefore, the influence of the bilayer physical state on the isomerization must be examined in terms of reaction rate, unlike in our previous paper. Eisenbach[19] similarly stated, in contrast with the previous finding of Paik and Morawetz,[20] that the conversion from *trans*- to *cis*-azobenzene at temperatures below the glass transition temperature (T_g) of a polymer matrix can be made the same as that attained at $T > T_g$, if irradiation times are long enough.

(18) Nakashima, N.; Ando, R.; Kunitake, T. *Bull. Chem. Soc. Jpn.* **1987**, *60*, 1967–1973.

(19) Eisenbach, C. D. *Makromol. Chem.* **1978**, *179*, 2489–2506.
(20) Paik, C. S.; Morawetz, H. *Macromolecules* **1972**, *5*, 171–177.

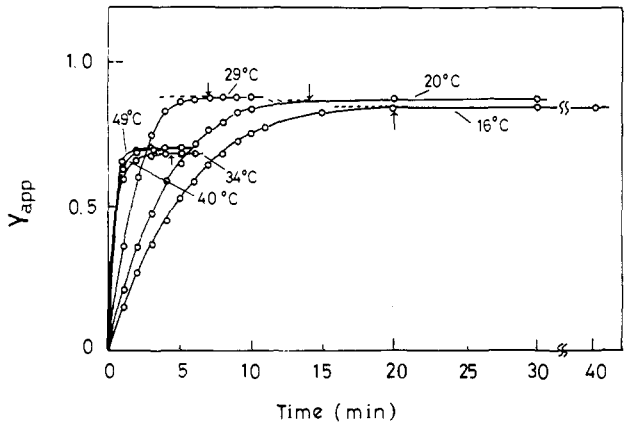

Figure 6. Time course of the trans-to-cis photoisomerization. $[C_{12}AzoC_5N^+] = 3.8 \times 10^{-4}$ M. The arrows indicate the photostationary state.

The apparent extent of photoisomerization (i.e., disappearance of the trans isomer) is determined by

$$Y_{app} = \frac{A_0 - A_t}{A_0} \quad (1)$$

where A_0 and A_t correspond to absorbances at 360 nm of the unirradiated (initial) and irradiated (time, t) states, respectively.

As shown in Figure 6, Y_{app} for the $C_{12}AzoC_5N^+$ bilayer levels off within a few minutes at 40–50 °C, but the changes are slower at lower temperatures. The initial rate estimated from the initial slope increases with temperature but becomes almost constant at ca. 34 °C. Since T_c of this aqueous bilayer is 32 °C, it is clear that the photostationary state is established very rapidly in the liquid-crystalline state.

The time required to reach the photostationary state was defined as the point of leveling off, as indicated by arrows in Figure 6. Similar experiments were conducted for other aqueous and nonaqueous (in ethanol) bilayers, and the results are summarized in Figure 7.

In ethanol the photostationary state is attained in ca. 2 min at all temperatures (10–40 °C). Azobenzene amphiphiles (e.g., $C_{12}AzoC_5N^+$) isolated in the $2C_{16}N^+2C_1$ matrix reach the photostationary state in similarly fast rates, independent of the reaction temperature. In contrast, strong temperature dependence is observed for single-component bilayers ($C_{12}AzoC_5N^+$ and $C_{10}AzoC_{10}N^+$). Their required times are close to those of isolated (in ethanol or in the bilayer matrix) azobenzenes at temperatures higher than the respective T_c's but become much longer as the temperature is lowered. It can be concluded that the photochemical reactivity of the liquid-crystalline azobenzene bilayers is analogous to that of the isolated bilayer components in ethanol or in the inert bilayer matrix.

The photoreactivity of the crystalline azobenzene bilayers is strongly affected by their chemical structures. In the crystalline states, the $C_{12}AzoC_5N^+$ bilayer isomerizes faster than the $C_{10}AzoC_{10}N^+$ bilayer, which, in turn, isomerizes faster than the $C_8AzoC_{10}N^+$ bilayer (data not shown). In fact, the last bilayer does not isomerize at all at 25 °C (T_c = 68 °C) even after 1 h of irradiation.

The Y value in the photostationary state (Y_∞) was determined more accurately by diluting the irradiated aqueous dispersions (250 μL) with 2.3 mL of ethanol in order to destroy the bilayer structure. This operation was required because spectral shapes of the bilayer dispersions are varied and the decrease in the 360-nm absorbance cannot be compared directly in the form of the aqueous bilayer.

The Y_∞ values are not extensively varied, except for the case of the aqueous $C_8AzoC_{10}N^+$ bilayer in which the Y value could not be estimated because of too slow reaction. The Y_∞ values are 0.83 to 0.86 in ethanol, and 0.70 to 0.77 in the single-component and matrix-buried azobenzene bilayers. The contrast between the constant Y value and the highly variable reaction rate will be discussed in the following section.

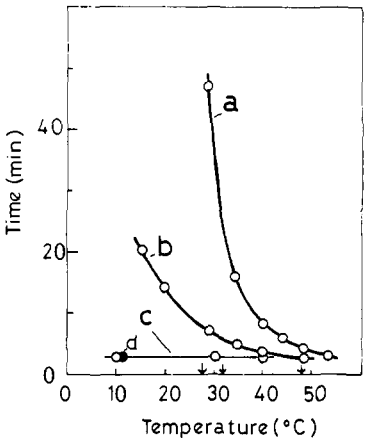

Figure 7. Temperature dependence of the reaction time required to reach the photostationary state: (a) aqueous $C_{10}AzoC_{10}N^+$ (T_c = 48 °C); (b) aqueous $C_{12}AzoC_5N^+$ (T_c = 32 °C); (c) aqueous mixture (molar ratio, 10:1) of $2C_{16}N^+2C_1$ and $C_{12}AzoC_5N^+$ (T_c of $2C_{16}N^+2C_1$ = 28 °C); (d) $C_{12}AzoC_5N^+$ in ethanol. The arrows indicate the locations of T_c.

Photoisomerization and Energy Transfer. The photoreactivity of the azobenzene bilayers is interestingly related to their spectroscopic properties. The single-component bilayer of $C_{12}AzoC_5N^+$ which shows a red shift (λ_{max} 370 nm) relative to the isolated azobenzene (λ_{max} 355 nm) isomerizes faster than the hypsochromic $C_{10}AzoC_{10}N^+$ bilayer (λ_{max} 330 nm). The most hypsochromic $C_8AzoC_{10}N^+$ bilayer (λ_{max} 300 nm) does not isomerize at all. As discussed in a previous section, the emission intensity increases with increasing bathochromic shifts of the absorption maximum. Therefore, the rate of the photoreaction correlates with changes of both absorption and emission spectra, implying that the reaction rate is closely related to the nature of the excited state that is peculiar to the bilayer assembly.

The fate of excitation energy, both chemical and physical, can be assessed by carrying out the photoisomerization in the absence and presence of a cyanine dye that acts as an energy acceptor. Without the cyanine dye (Figures 4 and 5), the trans-to-cis isomerization is induced by irradiation at 360 nm, and new absorption maxima due to the *cis*-azobenzene appear at ca. 450 nm. The emission from the *trans*-azobenzene bilayers (Figures 2 and 3) becomes weaker, as the isomerization progresses.

In the presence of the cyanine the emission pattern of the $C_{12}AzoC_5N^+$ bilayer is completely converted to that of the cyanine (Figure 3). Upon irradiation at 370 nm, the emission intensity monitored at 610 nm is lessened in concomitance with decrease in the absorption maximum at 370 nm. Curiously, however, the rates of decrease of these two spectra do not agree with each other. Figure 8 summarizes the time course of these decreases. The decrease in the trans isomer estimated from its absorbance is suppressed by addition of the cyanine. The suppression is not appreciable at cyanine concentrations of 1/29000 to 1/290 (mol/mol of azobenzene). When the cyanine concentration is enhanced to 1/59, the decrease levels off at only 6%. On the other hand, the emission intensity is lessened substantially at an early stage of the isomerization. At the molar ratio of 1/59, the intensity quickly reaches ca. 45% of the original value and remains the same upon prolonged irradiation. The decrease does not level off at smaller cyanine concentrations.

Two conclusions may be drawn from the data of Figure 8. First, the cyanine dye effectively inhibits the trans-to-cis photoisomerization (Figure 8a). Secondly, the energy transfer from the *trans*-azobenzene to the cyanine is suppressed by a small amount of the *cis*-azobenzene produced (Figure 8b). The cyanine inhibition of the trans-to-cis photoisomerization is supposedly attributed to the loss of the excitation energy due to transfer to the cyanine molecule and the subsequent emission. However, if the photochemically produced *cis*-azobenzene interferes with the energy transfer, the photoisomerization should not be suppressed by the cyanine at later stages of the reaction. This inconsistency

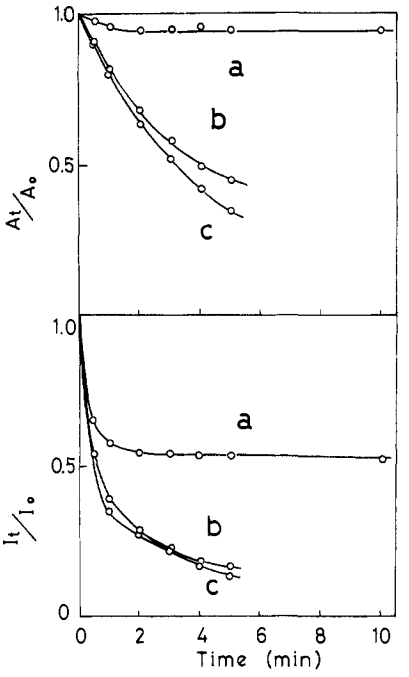

Figure 8. Intensity changes of absorption and emission spectra due to the trans-to-cis photoisomerization of the $C_{12}AzoC_5N^+$/cyanine system. $[C_{12}AzoC_5N^+] = 3.5 \times 10^{-4}$ M; 10 °C: (a) dye/membrane 1/59; (b) dye/membrane 1/290; (c) dye/membrane 1/2900. A_0 is the absorbance at 375 nm prior to photoisomerization. A_t is the absorbance at 375 nm at time t. I_0 is the emission intensity at 600 nm (excitation, 360 nm) prior to photoisomerization. I_t is the emission intensity at time t.

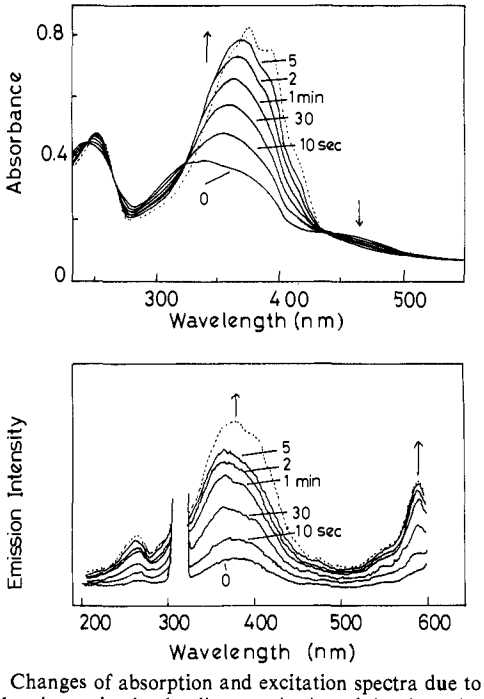

Figure 9. Changes of absorption and excitation spectra due to the cis-to-trans photoisomerization by direct excitation of the cis azobenzene at 450 nm. $[C_{12}AzoC_5N^+] = 3.5 \times 10^{-4}$ M; [cyanine 3] $= 1.2 \times 10^{-8}$ M; 10 °C. The excitation spectra are monitored at 610 nm. The broken-line spectra are obtained by incubation for 30 min after 5 min of irradiation.

is resolved if we assume that the cyanine acts as a photosensitizer of the cis-to-trans isomerization, as discussed below.

Cis-to-Trans Photoisomerization. Irradiation of the *cis*-azobenzene at 450 nm causes regeneration of the *trans*-azobenzene bilayer. Figure 9 illustrates the spectroscopic changes in the cis-to-trans isomerization process of the $C_{12}AzoC_5N^+$ bilayer. The cyanine dye, though present, is not involved in this photoisomerization process. The *trans*-azobenzene is rapidly regenerated

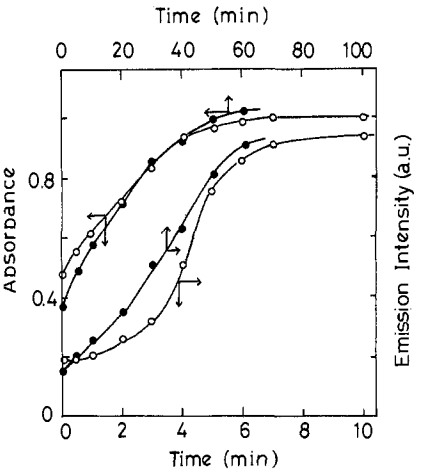

Figure 10. Intensity changes of absorption and emission spectra due to the dye-sensitized cis-to-trans photoisomerization. $[C_{12}AzoC_5N^+] = 3.5 \times 10^{-4}$ M; 10 °C; irradiation at 580 nm; (●) dye/membrane 1/2900; (○) dye/membrane 1/290. The absorbance increase at 375 nm (the trans isomer) and the relative emission recovery at 610 nm (Ex 360 nm) are used.

by the irradiation; however, the resulting absorption spectrum is centered at 360 nm and structureless. The structured peak characteristic of the head-to-tail orientation of azobenzene in the *trans*-$C_{12}AzoC_5N^+$ bilayer is produced only upon incubation in the dark for ca. 30 min. In the same vein, the recovery of the emission intensity is small immediately after the irradiation, and incubation is required to attain the full recovery. The fluorescence intensity is largest for the head-to-tail orientation, and without molecular reorganization to this orientation, it remains low. The recoveries of fluorescence emission and the head-to-tail *trans*-azobenzene proceed at similar rates.

It has been reported that dyes such as Rose Bengal and Eosin act as triplet sensitizers for the cis-to-trans photoisomerization of azobenzene.[21] Since the cyanine dye used here absorbs in a wavelength region similar to that of Rose Bengal, it may act as an energy donor to the *cis*-azobenzene bilayer. Consistent with this supposition, facile cis-to-trans isomerization was observed by irradiation at 580 nm where the cyanine absorbs but azobenzene does not. The structured absorption peak was recovered without incubation. The recovery of the *trans*-azobenzene was not significant in the *absence* of the cyanine dye under otherwise the same conditions (irradiation at 580 nm). The recovery of the emission is slower than that of the *trans*-azobenzene, as shown in Figure 10. This indicates that accumulation of the trans isomer precede the emission recovery. This result, together with the fact that the structured peak is regenerated without incubation, implies that the regenerated *trans*-azobenzene forms separate domains, unlike in the *unsensitized* cis-to-trans isomerization.

The inconsistency in the trans-to-cis isomerization mentioned in the previous section is now explicable in terms of the reverse reaction sensitized by the cyanine dye. In the initial stage of the reaction, the cyanine-sensitized isomerization produces a small amount of the cis isomer. Once formed, the cis isomer slows down further trans-to-cis isomerization not only by interference with the energy transfer process but also by the sensitized cis-to-trans isomerization. The latter process is especially crucial for maintenance of the photostationary state at a small fraction of the cis isomer.

Phase Separation and Photoisomerization. Azobenzene amphiphiles exist in the dialkylammonium bilayer matrix either in the isolated form or in the cluster form, depending on the component structure, temperature, and component ratios.[22-25]

(21) Ronayette, J.; Arnaud, R.; Lemaire, J. *Can. J. Chem.* **1974**, *75*, 1343-1347.
(22) Shimomura, M.; Kunitake, T. *Chem. Lett.* **1981**, 1001-1004.
(23) Shimomura, M.; Kunitake, T. *J. Am. Chem. Soc.* **1982**, *104*, 1757-1759.

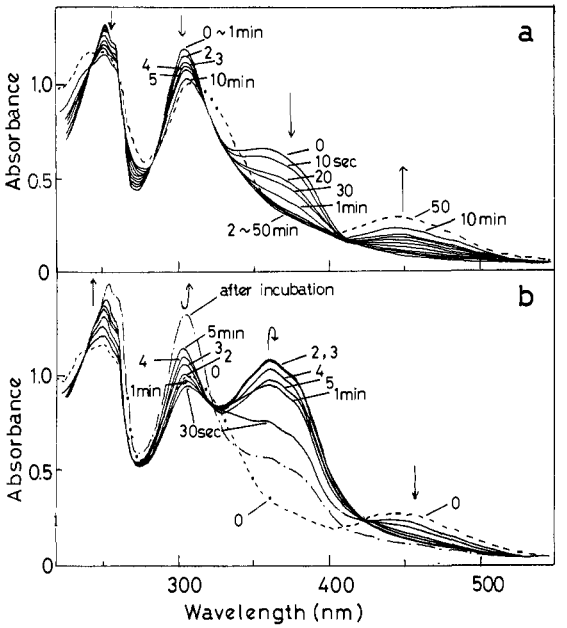

Figure 11. Photoisomerizations of an azobenzene bilayer in the $2C_{18}N^+2C_1$ matrix membrane. $[C_8AzoC_{10}N^+] = 7.5 \times 10^{-4}$ M; $[2C_{18}N^+2C_1] = 6.2 \times 10^{-3}$ M; 11 °C: (a) trans-to-cis photoisomerization (irradiation at 360 nm); (b) cis-to-trans photoisomerization (irradiation at 450 nm).

$C_{12}AzoC_5N^+$ usually exists as monomer in 10 times excess of the $2C_{16}N^+2C_1$ and $2C_{18}N^+2C_1$ bilayers without regard to phase transition of the matrices. Fluorescence emission is not observed under these conditions, because azobenzenes are isolated. The photostationary state for the monomeric azobenzene amphiphile is accomplished always rapidly within 2 min. The trans/cis ratio under these conditions does not depend on the matrix fluidity. Therefore, it is concluded that the photochemical behavior of the *monomeric* amphiphile is not detectably affected by the physical state of the matrix bilayer.

On the other hand, the monomeric species (λ_{max} 355 nm) of $C_8AzoC_{10}N^+$ is in equilibrium with the cluster species (λ_{max} 300 nm) in a 10 times excess of the $2C_{18}N^+2C_1$ bilayer matrix. As shown in Figure 11a, irradiation of the coexisting species at 360 nm leads to rapid disappearance of the 355-nm peak in the early stage (ca. 2 min), but the peak at 305 nm (the cluster species) starts to diminish more slowly after disappearance of the monomer species. The absorption of the cis isomer at ca. 450 nm increases concurrently with the decrease in the trans-isomer peak.

Figure 11b demonstrates spectral changes due to additional irradiation at 450 nm of the bilayer sample of Figure 11a. The peak of the monomeric trans isomer at 360 nm is regenerated rapidly by irradiation of the $n-\pi^*$ absorption of the cis isomer (450 nm). The recovery at 360 nm is greatest after 2 min and then the peak becomes smaller again. The cluster peak (300 nm) of the trans isomer decreases at the early stage of irradiation (30 s to 1 min) probably due to the decrease in the $\pi-\pi^*$ absorption of the cis isomer and then increases with the period of irradiation. When the sample solution is allowed to stand for 100 min in the dark after 5 min of irradiation, a further decrease in the monomer peak (360 nm) is observed along with an increase in the cluster peak. These changes are indicative of cluster formation of the regenerated trans isomer.

It is shown above that the single-component bilayer of $C_8AzoC_{10}N^+$ does not undergo photoreaction when irradiated at 360 nm. Its cluster species present in a bilayer matrix would be similarly unreactive, making direct conversion from the clustered trans isomer to the cis isomer not feasible. However, the reaction

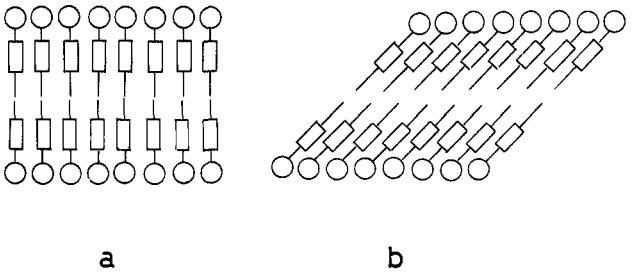

Figure 12. Schematic illustration of the component orientation in the azobenzene bilayer: (a) parallel chromophore orientation; (b) head-to-tail chromophore orientation.

Scheme I

clustered trans isomer $\overset{\text{equilibrium}}{\rightleftharpoons}$ monomeric trans isomer $\overset{360\text{ nm}}{\underset{450\text{ nm}}{\rightleftharpoons}}$ cis isomer (monomeric)

photoisomerization

proceeds since the unclustered (monomeric) amphiphile is present in equilibrium with the clustered species. As the trans-to-cis photoisomerization of the monomeric species proceeds, the trans monomer is provided from the cluster. These reaction pathways are illustrated in Scheme I. This scheme explains the reason why the amount of the monomeric trans species produced by the reverse (cis-to-trans) photoreaction (Figure 11a) is larger than that of the trans monomer prior to the trans-to-cis photoisomerization (Figure 11b). Because of the recovery of the trans monomer and the subsequent shift in equilibrium to the clustered species during the photoreversion process, the 355-nm absorption due to the trans monomer first increases and then decreases.

Discussion

Chromophore Orientation and Fluorescence. The photophysical and photochemical characteristics observed in this study are related to the orientation of the azobenzene chromophore in the bilayer assembly. We discussed in a previous paper the chromophore orientation on the basis of the absorption spectral characteristics.[6] The azobenzene units are in the head-to-tail orientation in the $C_{12}AzoC_5N^+$ bilayer, giving a bathochromic shift in absorption. The $C_8AzoC_{10}N^+$ bilayer, on the other hand, contains the azobenzene unit in the parallel orientation, which produces a hypsochromic shift. These situations are schematically represented in Figure 12.

The emission behavior of azobenzene and its derivatives has been examined by several investigators. Struve[26] conducted picosecond lifetime and depolarization studies of $^1(n,\pi^*)$ emission ($S_1 \rightarrow S_0$ emission) from unsubstituted *trans*-azobenzene and concluded a substantial contribution of fluorescence to the emission decay pattern with the decay time of ca. 25 ps. Morgante and Struve[27] subsequently reported that excitation in the $^1(\pi,\pi^*)$ manifold yielded an emission spectrum with a prominent $S_2 \rightarrow S_0$ fluorescence band of which decay at 420 nm is less than 5 ps, in addition to the $S_1 \rightarrow S_0$ component. Hamai and Hirayama[28] observed an $S_2 \rightarrow S_0$ fluorescence with λ_{max} at 385 nm and quantum yield of 1.7×10^{-5}. Its lifetime was estimated to be 0.06 ps. From the fluorescence behavior of azobenzenes adsorbed to powdered materials, Rau proposed that the criterion for their fluorescence ability is whether or not the (n,π^*) state lies higher in energy than the (π,π^*) state.[29]

It may be assumed based on these precedents that a predominant fraction of the emission from the azobenzene bilayers is fluorescence. Rau mentioned that triplet states have not so far been observed for any normal azo compounds by the usual spectroscopic methods.[30] A correlation observed between the

(24) Kunitake, T.; Ihara, H.; Okahata, Y. *J. Am. Chem. Soc.* **1983**, *105*, 6070–6078.
(25) Nakashima, N.; Morimitsu, K.; Kunitake, T. *Bull. Chem. Soc. Jpn.* **1984**, *57*, 3253–3257.
(26) Struve, W. S. *Chem. Phys. Lett.* **1977**, *46*, 15–19.
(27) Morgante, C. G.; Struve, W. S. *Chem. Phys. Lett.* **1979**, *68*, 267–271.
(28) Hamai, S.; Hirayama, F. *Annual Symposium on Photochemistry (Japan)*; 1984, Preprint, pp 315–316.
(29) Rau, H. *Ber. Bunsenges. Phys. Chem.* **1971**, *75*, 1343–1347.
(30) Rau, H. *Angew. Chem., Int. Ed. Engl.* **1973**, *12*, 224–235.

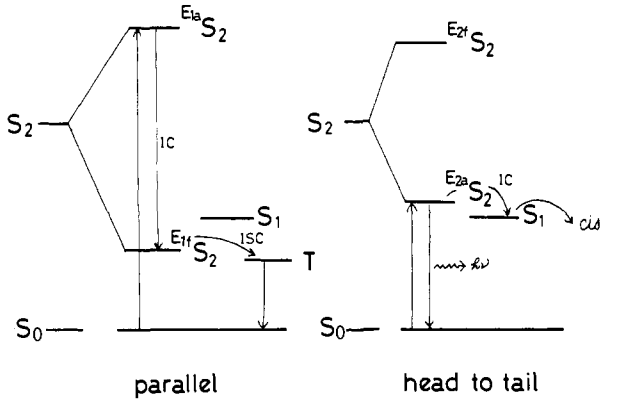

Figure 13. Energy level diagrams of azobenzene-containing bilayer membranes with different chromophore orientations.

absorption shift and the emission intensity (Figure 2) strongly suggests that the energy level of the excitonic state is directly related to fluorescence emission (and to the ease of photoisomerization). Figure 13 shows energy level diagrams that we propose for the bilayer assemblies that contain the azobenzene chromophore in the parallel or tilted (head-to-tail) arrangement. In the case of the parallel stacking, the excitonic level is split into two levels ($^{E1a}S_2$ and $^{E1f}S_2$) and the $S_2 \leftarrow S_0$ transition to the upper level is allowed. The internal conversion to the $^{E1f}S_2$ state would ensue. The relaxation of the latter to the ground S_0 state is forbidden. If the $^{E1f}S_2$ level is lower than the S_1 level, intersystem crossing to the T state would result. The S_0 state is regenerated by the radiationless decay from the T state. Neither photoisomerization from the S_1 state nor fluorescence from the S_2 state can proceed in these paths.

On the other hand, the excitation in the tilted arrangement is allowed to the lower S_2 level, which lies higher than the S_1 level. The excited $^{E2a}S_2$ molecule will relax by internal conversion to the S_1 state, from which the cis isomer is formed. Fluorescence from the S_2 state is also possible.

This scheme can explain qualitatively the above-mentioned, spectral and photoisomerization behavior of the bilayers of $C_{12}AzoC_5N^+$ (tilted stacking) and $C_8AzoC_{10}N^+$ (parallel stacking).

Photoisomerization. The efficiency of cis–trans photoisomerization is related to the chromophore orientation. The $C_{12}AzoC_5N^+$ bilayer which possesses the head-to-tail chromophore orientation isomerizes faster than the $C_8AzoC_{10}N^+$ bilayer which possesses the parallel chromophore orientation. Two kinds of explanation may be offered for the rate difference. One is the packing (volume) effect. Paik and Morawetz[20] reported that the cis fraction of the azobenzene unit in polymers in the photostationary state is smaller at temperatures below the glass transition temperature (T_g) than that at higher temperatures, although the difference may vanish after longer irradiation.[19] Whitten et al. mentioned that long-chain derivatives of thioindigo[31] and stilbazole[32] do not undergo trans–cis photoisomerization in builtup multilayers.

These results imply that mobility of the chromophores is crucial for efficient isomerization. It is true that the photoisomerization proceeds in the liquid-crystalline bilayer more readily than in the crystalline bilayer. The molecular reorganization accompanying photoisomerization will proceed more readily in the tilted packing of the half-bilayer in $C_{12}AzoC_5N^+$ than in the parallel, interdigitated structure of the $C_8AzoC_{10}N^+$ bilayer.

The other explanation is related to the fate of the excitation energy. The electronic mechanism of azobenzene isomerization is not yet fully understood. Rau and Lüddecke[33] proposed the inversion mechanism via the S_1 state ($n \rightarrow \pi^*$ excitation) on the basis of photoisomerization of an azobenzenophane. Monti et al.[34] estimated the energy surface of azobenzene isomerization by ab initio and configuration-interaction computations, proposing that the S_2 state derived by the $\pi \rightarrow \pi^*$ excitation undergoes internal conversion to the S_1 and S_0 state, the reaction occurring from the S_1 state.

In the bilayer system, the S_2 state is split into multiple levels, as illustrated in Figure 13. Photoisomerization would not proceed from the S_1 state, if the newly formed S_2 level is lower than the S_1 level. In the case of the $C_8AzoC_{10}N^+$ bilayer, the excitation is presumably allowed to a higher S_2 level that corresponds to a hypsochromic shift in absorption from 355 to 300 nm, and then the molecule relaxes to the lower S_2 level. The lower S_2 level to which the excitation is forbidden could be lower than the S_1 level that can lead to the S_0 level of the cis isomer. The photoisomerization would not proceed in this case. On the other hand, the electronic excitation of the $C_{12}AzoC_5N^+$ bilayer is allowed to the lower S_2 level, which is higher than the S_1 level, and photoisomerization can proceed.

As for the chemical mechanism, Taniguchi and co-workers[35] recently determined the activation parameters of the thermal cis-to-trans isomerization of a series of the azobenzene bilayers. The activation volume of the $C_{12}AzoC_{10}N^+$ bilayers was virtually zero, consistent with the inversion mechanism, but those of the other bilayers were in the range of 21–25 $cm^3\ mol^{-1}$, consistent with the rotation mechanism. The mechanism of the thermal process is not directly related to that of the photochemical process. However, it is probable that both of the rotation and inversion mechanisms could be involved also in the photochemical process due to varied structural characteristics of the bilayers.

Migration and Transfer of Excitation Energy. The excitonic state formed in the bilayer assembly is associated with energy migration among the chromophores. This is in fact consistent with highly efficient energy transfer to the cyanine dye and the concurrent suppression of the trans-to-cis photoisomerization. The singlet energy must be migrating in the process, since the cyanine molecules fluoresce.

Efficient energy migration in synthetic bilayer membranes was first suggested in the case of anthracene-containing membranes.[5] More recently, we found that fluorescence emission from bilayer membranes which possess the carbazole unit[36] and the naphthalene unit[37] is quenched by extremely small amounts of energy acceptors. For example, the fluorescence intensity of a carbazole-containing bilayer is lowered detectably by addition of $1/10^6$ mol/mol of perylenetetracarboxylate. Similar results are obtained in this study, since the fluroescence intensity of the $C_{12}AzoC_5N^+$ bilayer diminishes by addition of less than 1×10^{-6} mol/mol of a cyanine dye. We can conclude as more or less a general rule that organized chromophores in the bilayer assembly give rise to long-range electronic interactions.

The cis-to-trans photoisomerization by excitation of the doped cyanine will be attributed to the triplet sensitization. The transfer of the triplet energy usually occurs via the electron exchange (Dexter) mechanism, which is a short-range process compared with singlet energy transfer. Why then can a minute amount of the cyanine sensitize the cis-to-trans isomerization so effectively? It is improbable that the excited cyanine molecule travels around the bilayer surface to sensitize multiple azobenzene units.

In the sensitized photoreversion, the *trans*-azobenzene is regenerated as separate domains even without incubation (see Results). This implies that the recovery propagate from the site of doped cyanines. According to this mechanism, the triplet energy of the cyanine is transferred to a *cis*-azobenzene molecule and converts it to the trans configuration. The subsequent energy transfer from the cyanine molecule proceeds via the regenerated *trans*-azobenzene to the neighboring *cis*-azobenzene. When this process is repeated, arrays (or domains) of the *trans*-azobenzene

(31) Whitten, D. G. *J. Am. Chem. Soc.* **1974**, *96*, 594–596.
(32) Quina, F. H.; Whitten, D. G. *J. Am. Chem. Soc.* **1977**, *99*, 877–883.
(33) Rau, H.; Lüddecke, E. *J. Am. Chem. Soc.* **1982**, *104*, 1616–1620.
(34) Monti, S.; Orlandi, G.; Palmieri, P. *J. Chem. Phys.* **1982**, *71*, 87–99.
(35) Taniguchi, N., private communication.
(36) Kunitake, T.; Shimomura, M.; Hashiguchi, H.; Kawanaka, T. *J. Chem. Soc., Chem. Commun.* **1985**, 833–835.
(37) Nakashima, N.; Kimizuka, N.; Kunitake, T. *Chem. Lett.* **1985**, 1817–1820.

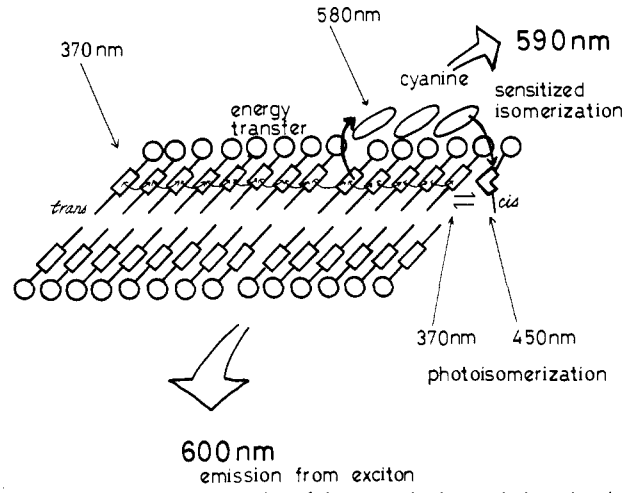

Figure 14. Schematic illustration of the photophysical and photochemical processes of an azobenzene-containing bilayer membrane.

will be formed instead of randomly distributed *trans*-azobenzenes, and efficient sensitization by the cyanine becomes possible.

Conclusion

Figure 14 summarizes schematically the photophysical and photochemical processes observed for the azobenzene bilayers with the $C_{12}AzoC_5N^+$ system as a typical example. Absorption at 370 nm produces an excitonic state which leads to isomerization directly or upon energy migration. The fluorescence emission at 600 nm also occurs from this state with enhanced quantum yield relative to that of the isolated species. Irradiation at 450 nm of the *cis*-azobenzene formed causes regeneration of the trans isomer. In the presence of bound cyanine dyes, the excitonic energy is transferred efficiently to the cyanine which subsequently fluoresces at 590 nm. Excitation of the cyanine at 580 nm results in the energy transfer to the *cis*-azobenzene and the consequent photoreversion to the trans isomer. The direct and sensitized photoreversions are contrasting in that the trans isomer is regenerated randomly in the former process, whereas it is regenerated in the cluster form in the latter case.

This scheme offers new possibilities in the construction of artificial photosynthetic systems. The photosynthetic system includes as major elements energy collection by antenna pigments, charge separation, and utilization of the charges for chemical reactions. The chromophore-containing bilayers can play the role of antenna pigments irrespective of whether the chromophores are bound to bilayers covalently or noncovalently. The charge separation can be accomplished when appropriate chromophores are introduced. We have shown that the positive hole created by photochemically induced electron transfer has an unexpectedly long lifetime in the case of a carbazole-containing bilayer.[38]

Monolayers and builtup multilayers have been used to prepare molecular systems that are capable of efficient transfer of energy and electron.[39,40] A large amount of work with planar lipid bilayers[41] and pigmented lipid bilayers also has been published.[42] It is clear that synthetic bilayer membranes provide molecular systems of similar capacity.[43]

Registry No. 3, 17701-26-7; **2** (n = 16), 42187-36-0; **2** (n = 18), 14357-21-2; $C_{12}AzoC_5N^+Br^-$, 88683-86-7; $C_{12}AzoC_6N^+Br^-$, 88683-87-8; $C_{12}AzoC_4N^+Br^-$, 88683-85-6; $C_{10}AzoC_{10}N^+Br^-$, 88683-82-3; $C_8AzoC_{10}N^+Br^-$, 88774-98-5.

(38) Takeyama, N.; Sakaguchi, H.; Hashiguchi, Y.; Shimomura, M.; Nakamura, H.; Kunitake, T.; Matsuo, T. *Chem. Lett.* **1985**, 1735-1738.
(39) Möbius, D. *Acc. Chem. Res.* **1981**, *14*, 63-68.
(40) For a recent attempt, see: Mooney, W. F.; Whitten, D. G. *J. Am. Chem. Soc.* **1986**, *108*, 5712-5719.
(41) Tien, H. T. *Bilayer Lipid Membranes (BLM): Theory and Practices*; Marcel Dekker: New York, 1974.
(42) Kalyanasundaram, K. *Photochemistry in Microheterogeneous Systems*; Academic: New York, 1987; Chapter 6.
(43) For a recent survey, see: Matsuo, T. *J. Photochem.* **1985**, *29*, 41-54.

Vinylidenecarbene: A New C_3H_2 Species

Günther Maier,*† Hans Peter Reisenauer,† Wolfgang Schwab,† Petr Čársky,‡,§ B. Andes Hess, Jr.,*‡ and Lawrence J. Schaad*‡

Contribution from the Institut für Organische Chemie der Justus-Liebig-Universität, D-6300 Giessen, West Germany, and the Department of Chemistry, Vanderbilt University, Nashville, Tennessee 37235. *Received February 17, 1987*

Abstract: It was found that photolysis of cyclopropenylidene in a matrix yields propargylene, which upon further irradiation is converted to a new C_3H_2 isomer. Comparison of the IR spectrum of this new isomer with the computed MP2/6-31G** IR spectrum of singlet vinylidenecarbene (ethenylidenecarbene, propadienylidene) confirms that this new C_3H_2 isomer has the structure $H_2C{=}C{=}C{:}$. The photolysis can be reversed by using shorter wavelength light to regenerate propargylene.

The experimental search for isomers on the C_3H_2 potential surface (e.g., **1**-**3**) began about 20 years ago with the trapping of the diphenyl derivative of cyclopropenylidene by dimethyl fumarate and dimethyl maleate.[1] The first C_3H_2 parent species identified by direct spectroscopic methods was triplet propargylene (**2**). In 1965 the ESR spectrum of **2** was published; and, based on the zero-field-splitting parameters, a linear or nearly linear structure was derived.[2] In 1972 a matrix-isolation study on the photolysis of diazopropyne and the IR spectrum of the same species was reported.[3] In 1974 **2** was identified as one of the products of the vacuum UV photolysis of matrix-isolated propyne and allene.[4] Some years later[5] the existence of a C_3H_2 species with a high proton affinity was claimed to be present in hydrocarbon flames on the basis of an ion cyclotron resonance study, but no

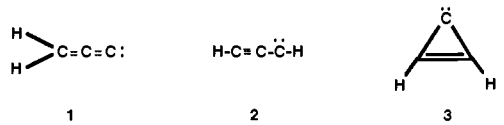

1 **2** **3**

† Justus-Liebig-Universität.
‡ Vanderbilt University.
§ Permanent address: J. Heyrovský Institute of Physical and Electrochemistry, Czechoslovak Academy of Sciences, Máchova 7, 121 38 Prague 2, Czechoslovakia.

(1) Jones, W. M.; Stowe, M. E.; Wells, E. E., Jr.; Lester, E. W. *J. Am. Chem. Soc.* **1968**, *90*, 1849.
(2) Bernheim, R. A.; Kempf, R. J.; Gramas, J. V.; Skell, P. S. *J. Chem. Phys.* **1965**, *43*, 196.
(3) Chi, F. K., Dissertation, Michigan State University, 1972.
(4) Jacox, M. E.; Milligan, D. E. *Chem. Phys.* **1974**, *4*, 45.
(5) McAllister, T.; Nicholson, A. J. C. *J. Chem. Soc., Faraday Trans. 1* **1981**, *77*, 821.

0002-7863/87/1509-5183$01.50/0